

Ab Initio Investigation of Proton Transfer in Ammonia–Hydrogen Chloride and the Effect of Water Molecules in the Gas Phase

Robert A. Cazar, Alan J. Jamka, and Fu-Ming Tao*

Department of Chemistry and Biochemistry, California State University, Fullerton, Fullerton, California 92834

Received: February 11, 1998; In Final Form: April 17, 1998

The gas-phase proton-transfer reaction of ammonia–hydrogen chloride and the effect of the first three water molecules are investigated by high-level ab initio calculations on the molecular clusters $\text{NH}_3\text{--HCl--}(\text{H}_2\text{O})_n$, $n = 0, 1, 2, 3$. The equilibrium structures, binding energies, and harmonic frequencies of the clusters as well as the potential energy surfaces along the proton-transfer pathway of ammonia–hydrogen chloride are calculated at the second-order Møller–Plesset perturbation (MP2) level with the extended basis set 6-311++G(d,p). Either without water or with one water molecule, the ammonia–hydrogen chloride system exists as a usual hydrogen-bonded complex. With two or three water molecules, the system becomes an ion pair resulting from the complete transfer of a proton from hydrogen chloride to ammonia. The potential energy surfaces along the proton-transfer pathway are examined to understand the effect of the water molecules. The harmonic frequencies and infrared intensities of the clusters provide additional evidence in support of the transition from the hydrogen bond to the ion pair structure as the water molecules are stepwise introduced. On the basis of these results, we conclude that ammonium chloride might be formed by the gas-phase reaction of hydrogen chloride with ammonia in the presence of adequate water vapor.

1. Introduction

Transfer of a proton from one atom to another is one of the most general and important processes in chemistry. This elementary process plays a crucial role in a wide range of chemical and biological reactions, from simple acid–base neutralization to tautomeric interconversion in DNA bases. The understanding of such a process has for a long time attracted wide attention from all areas across chemistry. Ammonia and hydrogen chloride ($\text{NH}_3\text{--HCl}$) provide us with a simple, prototypical acid–base pair for studying proton-transfer reactions. In the aqueous solution, the reaction of HCl with NH_3 is instantaneous, and forms the solvated ions, $\text{NH}_4^+\cdots\text{Cl}^-$, as the product. One may, however, puzzle over the following questions: what is the detailed mechanism of proton transfer and what is the stable form of $\text{NH}_3\text{--HCl}$ in the gas phase? Mulliken^{1,2} speculated that gas-phase $\text{NH}_3\text{--HCl}$ might exist as an ion pair ($\text{NH}_4^+\cdots\text{Cl}^-$) just as in the aqueous solution. Early ab initio calculations by Clementi^{3–5} indeed showed the strong ion-pair character for the system. These seem to corroborate with the well-known observation that a white fog of solid ammonium chloride particles appears in the interdiffusion of the vapors from concentrated ammonia and hydrochloric acid.^{6,7} However, microwave experiments by Legon and co-workers^{8,9} concluded that the system exists as a simple hydrogen-bonded complex with HCl as the hydrogen bond donor and NH_3 as the acceptor rather than an ion pair form resulting from complete proton transfer. This experimental result is supported by several higher level ab initio calculations^{10–15} and by matrix isolation studies.¹⁶

The experimental and theoretical studies carried out thus far have focused on the pure binary system of $\text{NH}_3\text{--HCl}$, although Legon and co-workers^{17–19} studied many other acid–base systems and observed proton transfer in several gas-phase $\text{N}(\text{CH}_3)_3\text{--HX}$ systems. We anticipate water to play a critical

role in assisting proton transfer in $\text{NH}_3\text{--HCl}$ and in the majority of other acid–base systems. In fact, self-consistent reaction field (SCRf) calculations¹³ of aqueous $\text{NH}_3\text{--HCl}$ gave the stable ion pair product as expected. All of the SCRf methods,^{20,21} however, treated $\text{NH}_3\text{--HCl}$ as a solute in a cavity which is surrounded by a continuum characterized by the dielectric permittivity of liquid water, and therefore no details were given about the specific solute–solvent interactions in the framework of the continuum model. As a result, the exact role played by the individual water molecules and the detailed mechanism of proton transfer in $\text{NH}_3\text{--HCl}$ were not delineated. More specifically, it is not clear whether proton transfer must take place in the aqueous solution or whether it is possible in the gas phase in the presence of only a few water molecules (water vapor). If the latter is true, then what is the minimum number of water molecules involved in proton transfer in $\text{NH}_3\text{--HCl}$? What is the exact role played by each water molecule? What are the structural relationships among the ions and the water molecules in the system, and what are the molecular properties characteristic of the system?

In this paper, we attempt to provide some of the answers to these questions from high-level ab initio calculations on the four molecular clusters, $\text{NH}_3\text{--HCl--}(\text{H}_2\text{O})_n$ ($n = 0, 1, 2, 3$). We compute the equilibrium structures, vibrational frequencies, and binding energies of the clusters as well as the potential energy curves along the $\text{NH}_3\text{--HCl}$ proton-transfer reaction pathway. As one of the main goals of this study, we wish to explore whether proton transfer is possible for the $\text{NH}_3\text{--HCl}$ system in the presence of only a few water molecules. If proton transfer is possible, we will then determine the minimum number of water molecules involved in the $\text{NH}_3\text{--HCl}$ proton transfer and study the role of these water molecules individually. We also wish to discuss some interesting theoretical predictions that would stimulate and guide new experiments on the relevant problems. Finally, we hope that the results of this study will

be instructive in understanding the general mechanism for acid–base proton-transfer reactions.

2. Theoretical Method

Equilibrium geometries for the clusters, $\text{NH}_3\text{--HCl--}(\text{H}_2\text{O})_n$ ($n = 0, 1, 2, 3$), were obtained by full geometry optimization at the level of frozen-core second-order Møller–Plesset perturbation approximation (MP2),^{22,23} with the extended basis set 6-311++G(d,p).^{24–26} Harmonic vibrational frequencies and infrared intensities of the equilibrium geometries were also obtained at the MP2/6-311++G(d,p) level using analytical force constants. We searched for the equilibrium geometries at other intermolecular configurations with competitive stability, but all were eventually optimized to the same global minimum geometries as reported. The intermolecular energies in $\text{NH}_3\text{--HCl--}(\text{H}_2\text{O})_n$ ($n = 0, 1, 2$, or 3) are expected to be dominated by exchange and electrostatic energies which are readily recovered at the Hartree–Fock level. Consequently, electron correlation at the MP2 level should be sufficient for the recovery of the relatively small dispersion energy.

The binding energy D_e of each cluster was given as a difference between the total energy of the cluster and the sum of the total energies of the isolated monomeric species (hydrogen chloride, ammonia, and water) present in the cluster. The zero-point energy (ZPE) corrections based on harmonic vibrational frequencies were also considered to give the ZPE-corrected binding energy D_0 of the cluster. It should be noted that the basis set superposition error (BSSE) was not considered in the present study. A reliable estimate of BSSE for a reacting molecular system involving several interacting submolecules such as those involved in this work is a rather difficult issue, and might not be possible because of the lack of a unique and consistent reference for defining the BSSE. This is particularly true when multiple water molecules are involved. Fortunately, as shown in our previous study,²⁷ the BSSE effect on D_e for a similar system ($\text{HNO}_3\text{--NH}_3$) at the equilibrium geometry was found to be less than 0.4 kcal/mol with the 6-311++G(d,p) basis set, which may be regarded as negligible compared to the binding energy of $\text{HNO}_3\text{--NH}_3$ (about 14 kcal/mol). This indicates that the BSSE effect in the present study is negligibly small with the 6-311++G(d,p) basis set.

The potential energy surface of each cluster along the proton-transfer pathway of $\text{NH}_3\text{--HCl}$ was calculated with a constrained optimization procedure. Only the H–Cl bond distance was constrained while the geometry of the cluster was optimized. The potential energy surface was scanned at a set of values for the H–Cl bond distance with variable increments, and was represented by the energy of each cluster as a function of the H–Cl bond distance.

All calculations were carried out with the Gaussian 94 program package^{28,29} on DEC Alpha 5/266 and IBM RS6000/3CT workstations running Digital UNIX and AIX, respectively.

3. Results and Discussion

Equilibrium Structures. A schematic structure showing the $\text{NH}_3\text{--HCl}$ unit surrounded by one H_2O molecule is presented in Figure 1, along with the labeling of the atoms. The cluster structures with two and three H_2O molecules may be formed by stepwise addition of H_2O to the $\text{NH}_3\text{--HCl}$ unit so that the H_2O being added occupies the remaining positions with C_{3v} symmetry about the principal axis of $\text{NH}_3\text{--HCl}$. Each of the H_2O molecules is exactly coplanar with one of the three H–N–Cl planes in $\text{NH}_3\text{--HCl}$, except for $\text{NH}_3\text{--HCl--}(\text{H}_2\text{O})_2$ case in which one H_2O is slightly drifted out of the plane after geometry

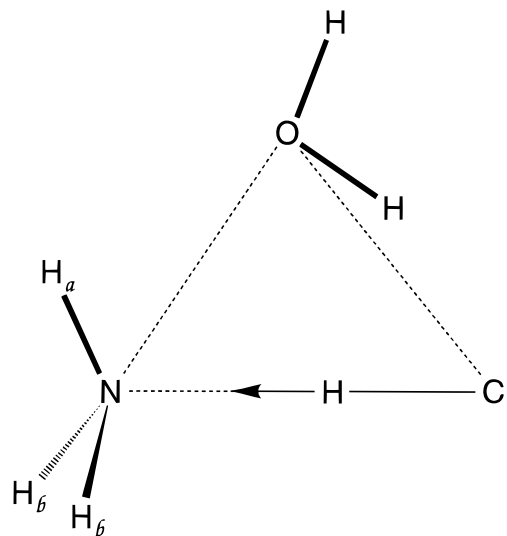


Figure 1. A schematic cluster structure of $\text{NH}_3\text{--HCl}$ surrounded by one H_2O molecule and the labeling of the atoms. Cluster structures with two and three H_2O molecules may be constructed by stepwise addition of H_2O at the remaining positions with C_{3v} symmetry about the principal axis of $\text{NH}_3\text{--HCl}$. The arrow shows the direction of the proton transfer in $\text{NH}_3\text{--HCl}$ as the H_2O molecules are added.

TABLE 1: Equilibrium Bond Lengths (in Å), Bond Angles (degrees), Dipole Moments μ (D), and Total Energies (Hartrees) of NH_3 , HCl , H_2O , and NH_4^+ from MP2 Calculations with the 6-311++G(d,p) Basis Set

molecule ^a (symmetry)	parameter	[MP2]	expt ^b
NH_3 (C_{3v})	$r(\text{NH})$	1.014	1.012
	$\angle\text{HNH}$	107.2	107.0
	μ	1.74	1.47
	$E(\text{SCF})$	−56.21428	
	$E(\text{MP2})$	−56.41552	
HCl	$r(\text{HCl})$	1.273	1.275
	μ	1.37	1.11
	$E(\text{SCF})$	−460.09548	
	$E(\text{MP2})$	−460.24492	
	H_2O (C_{2v})	$r(\text{OH})$	0.960
$\angle\text{HOH}$		103.5	104.5
μ		2.26	1.85
$E(\text{SCF})$		−76.05260	
$E(\text{MP2})$		−76.27492	
NH_4^+ (T_d)	$r(\text{NH})$	1.024	
	$E(\text{SCF})$	−56.55865	
	$E(\text{MP2})$	−56.75569	

^a Some of the atomic labels are omitted due to uniqueness or symmetry. ^b Experimental equilibrium structures for NH_3 and H_2O are from ref 30 and for HCl from ref 31; experimental dipole moments are from ref 32.

optimization, which is likely the result of the repulsion from the other H_2O molecule. The bond distances, bond angles, dipole moments, and total energies of the monomeric species, NH_3 , HCl , H_2O , and NH_4^+ , are presented in Table 1 and compared with the available experimental values.^{30–32} The three-dimensional structures of the clusters are shown in Figure 2 with two side views of each cluster. The selected bond distances, rotational constants, and dipole moments of the clusters are presented in Table 2.

It is clear from Table 1 that the calculated geometries of the monomers and their properties are all in reasonable agreement with experimental values. All bond lengths fall within 0.005 Å and the bond angles within 0.5° from experiment. The calculated dipole moments, particularly at the self-consistent field (SCF) level, are larger than the experimental values. This is typical for the level of theory and basis set used in this study.

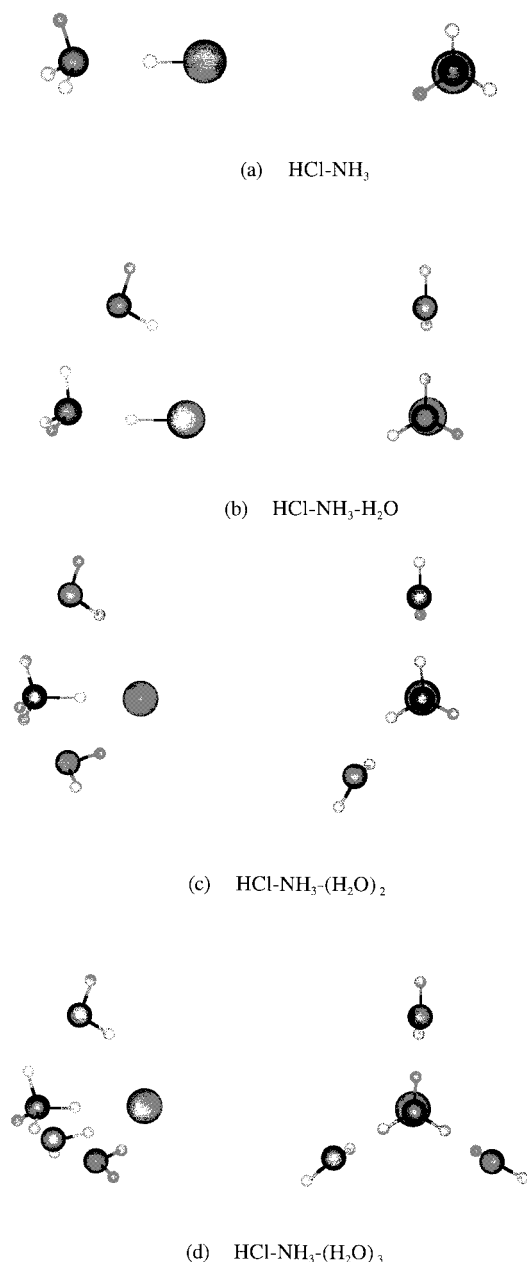


Figure 2. Two side views of the equilibrium structure for each of the clusters (a) NH₃-HCl, (b) NH₃-HCl-H₂O, (c) NH₃-HCl-(H₂O)₂, and (d) NH₃-HCl-(H₂O)₃.

The large dipole moments may potentially lead to an overestimation of the binding energy in weakly bonded complexes. However, the contribution of dipole-dipole interaction to the binding energy in the complexes is less important than the contributions of high multipole interactions. This can be seen by comparing the SCF and MP2 values of the dipole moments with those of the binding energies (see D_e values in Table 3). The SCF values of the dipole moments are more severely overestimated, but the SCF values of the binding energies are about 50% less than the MP2 values. The calculated proton affinity (PA) based the SCF or MP2 energies of NH₃ and NH₄⁺ listed in the table is about 10 kcal/mol too large compared to the experimental value of 205 kcal/mol,³³ but the correction for zero-point vibrations, 9.5 kcal/mol, brings the calculated PA in nearly complete agreement with the experiment.

It is clear from the cluster structures presented in Figure 2 and Table 2 that, either without H₂O or with one H₂O molecule, the NH₃-HCl unit is hydrogen-bonded, with HCl acting as the

TABLE 2: Selected Equilibrium Bond Lengths (in Å), Bond Angles (degrees) Rotational Constants A, B, C (GHz), and Dipole Moments μ (D) of NH₃-HCl-(H₂O)_n (n = 0, 1, 2, 3) from MP2/6-311++G(d,p) Calculations

parameter	NH ₃ -HCl	NH ₃ -HCl-H ₂ O	NH ₃ -HCl-2H ₂ O	NH ₃ -HCl-3H ₂ O
$r(\text{H}-\text{Cl})$	1.312 ^a	1.361	1.861	1.938
$r(\text{N}\cdots\text{H})$	1.820 ^a	1.613	1.087	1.062
$r(\text{N}-\text{H}_a)$	1.016	1.016	1.026	1.022
$r(\text{N}\cdots\text{Cl})$	3.132 ^{a,b}	2.966	2.922	3.000
$r(\text{N}\cdots\text{O})$		2.943	2.739	2.767
$r(\text{Cl}\cdots\text{O})$		3.322	3.120	3.178
$\angle\text{HNH}_a$	112.1	115.1	104.9	106.2
$\angle\text{H}_a\text{NH}_b$	106.7	108.0	111.5	112.5
$\angle\text{NHCl}$	180.0	171.7	164.2	180.0
A	188.762	6.313	3.359	1.648
B	4.247 ^b	3.531	2.393	1.648
C	4.247	2.292	1.659	1.397
μ	4.648	3.470	6.038	4.181

^a CCSD(T) values (ref 15): $r(\text{N}\cdots\text{Cl}) = 3.137$ Å, $r(\text{H}-\text{Cl}) = 1.302$ Å, and $r(\text{N}\cdots\text{H}) = 1.835$ Å. ^b Experimental values (ref 9): $r(\text{N}\cdots\text{Cl}) = 3.136$ Å, $B = 4.243$ GHz.

hydrogen bond donor and NH₃ as the acceptor. The optimized geometry for NH₃-HCl without H₂O has C_{3v} symmetry as expected. The hydrogen bond distance, $r(\text{N}\cdots\text{H}) = 1.820$ Å, is approximately the same as the CCSD(T) value of 1.835 Å by Corongiu et al.¹⁵ It is shorter than the hydrogen bond distance in a more typical hydrogen-bonded system such as in the water dimer (1.96 Å), indicating a strong hydrogen bond between NH₃ and HCl. The heavy atom distance, $r(\text{N}\cdots\text{Cl}) = 3.132$ Å, and the rotational constant, $B = 4.247$ GHz, are in excellent agreement with the experimental values, 3.136 Å and 4.247 GHz, respectively.⁹ In NH₃-HCl-H₂O, the C_{3v} symmetry of NH₃-HCl is broken and the hydrogen bond in NH₃-HCl is bent as shown by the angle $\angle\text{NHCl} = 171.7^\circ$. The H₂O molecule is coplanar with N-Cl-H of NH₃-HCl-H₂O, indicating that H₂O is not hydrogen bonded with NH₃. The hydrogen bond distance between NH₃ and HCl, $r(\text{N}\cdots\text{H})$, decreases from 1.820 Å in NH₃-HCl to 1.613 Å in NH₃-HCl-H₂O, but the bond distance of HCl, $r(\text{H}-\text{Cl})$, increases from 1.312 to 1.361 Å. This indicates further strengthening of the strong hydrogen bond in NH₃-HCl, but weakening of the H-Cl bond occurs because of the presence of the H₂O molecule. The three heavy atoms, N, Cl, and O, approximately located at the centers of mass for the three molecules in the cluster, form a nearly equilateral triangle as shown by the distances $r(\text{N}\cdots\text{Cl})$, $r(\text{N}\cdots\text{O})$, and $r(\text{Cl}\cdots\text{O})$.

The structure of the NH₃-HCl unit changes dramatically in the presence of two H₂O molecules. The second H₂O takes a position symmetrically equivalent to the first molecule around NH₃-HCl, but is slightly off plane formed by a second N-H bond and the N \cdots Cl axis of the NH₃-HCl unit, which is probably due to the repulsion between the two H₂O molecules. The major structural change in NH₃-HCl due to the presence of the second H₂O is the increase of the bond distance $r(\text{H}-\text{Cl})$ from 1.361 to 1.861 Å and the decrease of the bond distance $r(\text{N}\cdots\text{H})$ from 1.613 to 1.087 Å. This indicates that the H-Cl bond is no longer existent and a new N-H bond is formed. In other words, a proton is transferred from HCl to NH₃, forming an ion pair, NH₄⁺ \cdots Cl⁻. The formation of such an ion pair is also demonstrated by a sharp increase in the dipole moment (from 3.47 to 6.04 D) from the one-water to the two-water cluster.

In NH₃-HCl-(H₂O)₃, the third H₂O takes a position so that the C_{3v} symmetry in pure NH₃-HCl is restored after geometry optimization. The third H₂O effectively moves the transferred

TABLE 3: Hartree-Fock SCF and MP2 Total Energies (in Hartrees) and Binding Energies D_e (kcal/mol), MP2 Zero-Point Energy Corrections ΔZPE (kcal/mol), and ZPE-Corrected Binding Energies D_0 (kcal/mol) of $\text{NH}_3\text{-HCl-}n\text{H}_2\text{O}$ ($n = 0,1,2,3$)

molecule	$E(\text{SCF})^a$	$E(\text{MP2})$	$D_e(\text{SCF})^a$	$D_e(\text{MP2})$	ΔZPE	$D_0(\text{MP2})$
$\text{NH}_3\text{-HCl}^{b,c}$	-516.31973	-516.67520	6.24	9.26	-2.61	6.65
$\text{NH}_3\text{-HCl-H}_2\text{O}$	-592.37788	-592.96256	9.73	17.07	-4.51	12.56
$\text{NH}_3\text{-HCl-(H}_2\text{O)}_2$	-668.45159	-669.25879	22.97	30.44	-9.83	20.61
$\text{NH}_3\text{-HCl-(H}_2\text{O)}_3$	-744.52154	-745.55328	33.87	42.72	-11.58	31.14

^a The SCF total energies and binding energies are reported for the MP2 equilibrium structures. ^b Experimental value for $\text{NH}_3\text{-HCl}$: $D_0 = 8.0 \pm 2.8$ kcal/mol (ref 34). ^c CCSD(T) values for $\text{NH}_3\text{-HCl}$: $D_e = 8.0$ kcal/mol, $D_0 = 5.5$ kcal/mol (ref 15).

proton closer to the nitrogen. The $r(\text{H-Cl})$ distance increases by 0.077 Å to 1.938 Å, whereas $r(\text{N}\cdots\text{H})$ decreases by 0.027 Å to 1.062 Å. Nevertheless, the geometry of the $\text{NH}_3\text{-HCl}$ unit is similar to that with two H_2O molecules. It is reasonable to expect no major structural changes for the $\text{NH}_3\text{-HCl}$ unit when more than three water molecules are brought into the system.

It is interesting to note that the dipole moment of the three-water cluster is decreased upon the addition of the third water molecule, in contrast to the sharp increase in the dipole moment from the one-water to the two-water cluster. This result may be explained by the fact that all of the water monomer dipole moments in the cluster are aligned by the electrostatic forces in the direction to cancel out the dipole moment contribution from the $\text{NH}_3\text{-HCl}$ unit. The decrease, from 6.04 to 4.18 D, is approximately accountable by the component dipole of the third water (≈ 2.0 D) and the realignment of the overall dipole of the cluster along the C_{3v} axis. In fact, a similar decrease in the dipole moment is also seen as the first water molecule is added to the $\text{NH}_3\text{-HCl}$ unit without transfer of a proton. The decrease due to the first water, from 4.65 to 3.47 D, is smaller in magnitude than the decrease due to the third water. This may be attributed to the water dipole contribution in the direction off the $\text{NH}_3\text{-HCl}$ axis in $\text{NH}_3\text{-HCl-H}_2\text{O}$. As a result, the varying dipole moments of the clusters may be sufficiently explained by a simple vector model and there are no substantial polarizations within the subunits of the clusters.

Binding Energies and Potential Energy Surfaces. The total energies and binding energies of the clusters are summarized in Table 3, along with the ZPE corrections and ZPE-corrected binding energies. As shown in the table, the binding energy of a cluster (with respect to the infinitely separate monomers HCl , NH_3 , and H_2O) increases progressively with the number of H_2O molecules in the cluster. The binding energy D_e (MP2) for $\text{NH}_3\text{-HCl}$ without water is 9.26 kcal/mol, which is compared to the CCSD(T) value of 8.0 kcal/mol by Corongiu et al.¹⁵ The ZPE correction is -2.61 kcal/mol, which leads to the ZPE-corrected binding energy $D_0 = 6.65$ kcal/mol. This value is between that of CCSD(T), 5.5 kcal/mol,¹⁵ and that of the experiment, 8.0 ± 2.8 kcal/mol.³⁴ Compared to more typical hydrogen-bonded complexes such as water dimer, the binding energy for $\text{NH}_3\text{-HCl}$ is much larger, and is consistent with the shorter hydrogen bond distance in $\text{NH}_3\text{-HCl}$ discussed in the earlier section.

The presence of the first H_2O results in an increase of about 8 kcal/mol in D_e . This energy change can be viewed as the hydration energy of $\text{NH}_3\text{-HCl}$ by a single water molecule. The introduction of the second and the third H_2O molecules each results in an increase of about 13 kcal/mol in D_e . This is much larger than the increase in D_e due to the first H_2O molecule added. This indicates that the hydration by the first H_2O is somewhat different from that by the second or the third H_2O . Such a difference in hydration energy might suggest that the species being hydrated are physically different in their interac-

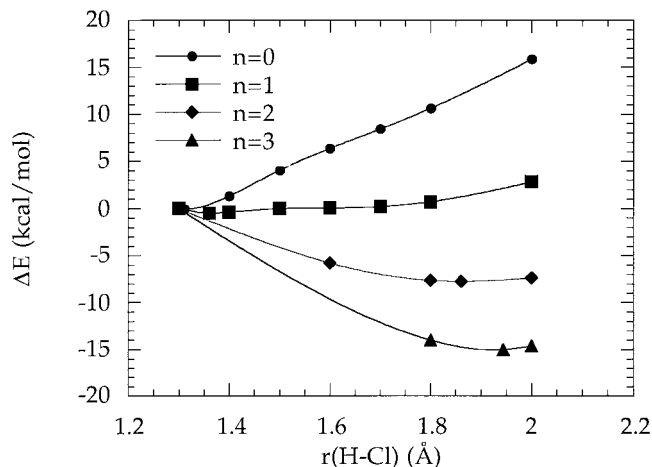


Figure 3. Potential energy profiles along the proton-transfer pathway of $\text{NH}_3\text{-HCl}$ in the clusters $\text{NH}_3\text{-HCl-(H}_2\text{O)}_n$, $n = 0, 1, 2, 3$. The energy ΔE (in kcal/mol) of each cluster is relative to that of the cluster with $r(\text{H-Cl}) = 1.3$ Å.

tions with water molecules. The $\text{NH}_3\text{-HCl}$ with the first H_2O is a neutral hydrogen-bonded complex, but with two or three H_2O molecules it becomes an ion pair. Generally, an ionic species is more readily hydrated with a larger hydration energy than is a neutral species.

The D_e values at the SCF level range from about 57% of the D_e at MP2 for $\text{NH}_3\text{-HCl-H}_2\text{O}$ to 80% for $\text{HCl-NH}_3\text{-(H}_2\text{O)}_3$. It indicates that the binding energies appear to be predominated by electrostatic interactions, particularly for the clusters containing the ion pair.

To understand the onset of proton transfer in the series $\text{NH}_3\text{-HCl-(H}_2\text{O)}_n$ ($n = 0, 1, 2, 3$) and the role of the water molecules, we now examine the potential energy surface along the proton-transfer pathway between HCl and NH_3 and its change with an increasing number of water molecules. The minimum energy curves along the proton-transfer pathway for the clusters $\text{NH}_3\text{-HCl-(H}_2\text{O)}_n$ ($n = 0, 1, 2, 3$) are presented in Figure 3, in which the energy of each cluster, relative to the energy at $r(\text{H-Cl}) = 1.3$ Å, is plotted as a function of $r(\text{H-Cl})$.

For $\text{NH}_3\text{-HCl}$ without H_2O , the potential energy minimum is located near $r(\text{H-Cl}) = 1.3$ Å and corresponds to a hydrogen-bonded structure. As the proton is forced to transfer to the nitrogen of NH_3 , the energy of $\text{NH}_3\text{-HCl}$ increases sharply. This indicates that proton transfer is unlikely in pure $\text{NH}_3\text{-HCl}$, and the ion pair structure is unstable with respect to the hydrogen-bonded structure. For $\text{NH}_3\text{-HCl-H}_2\text{O}$, the potential minimum is also located near $r(\text{H-Cl}) = 1.3$ Å and the system remains hydrogen-bonded. However, the potential energy curve for $\text{NH}_3\text{-HCl-H}_2\text{O}$ becomes much flatter than that of $\text{NH}_3\text{-HCl}$. This indicates that the ion pair form becomes close in stability to the hydrogen bond form of $\text{NH}_3\text{-HCl-H}_2\text{O}$. We therefore conclude that the H_2O molecule favors the stability of the ion pair over the hydrogen bond form as it creates a flat potential energy pathway for proton transfer.

TABLE 4: Harmonic Vibrational Frequencies (in cm^{-1}) and Infrared Intensities (km/mol) of $\text{NH}_3\text{--HCl}$ and $\text{NH}_3\text{--HCl--H}_2\text{O}$ Correlated by Intramolecular Vibrational Modes for NH_3 , HCl , and H_2O^a

monomer	mode	isolated monomers		$\text{NH}_3\text{--HCl}$		$\text{NH}_3\text{--HCl--H}_2\text{O}$	
		freq	IR int	freq	IR int	freq	IR int
NH_3^b	ν_1 sym str	3526 (3506)	2	3514	0	3490	31
	ν_2 sym deform	1073 (1022)	206	1171	135	1197	88
	ν_3 <i>d</i> -str	3678 (3577)	6	3655	17	3627	69
					3659	21	
	ν_4 <i>d</i> -deform	1666 (1691)	24	1637	24	1645	19
						1648	25
HCl^c	ν_1 str	3091 (2990)	35	2528	1572	1901	2888
H_2O^d	ν_1 sym str	3884 (3832)	13			3829	79
	ν_2 antisym str	4003 (3943)	63			3978	121
	ν_3 bend	1629 (1648)	57			1652	137

^a Experimental harmonic frequencies for the monomers are given in parentheses. Intermolecular frequencies and IR intensities are listed in Supporting Information. ^b Experimental harmonic frequencies for NH_3 are from ref 35. ^c Experimental harmonic frequency for HCl is from ref 31. ^d Experimental harmonic frequencies for H_2O are from ref 36.

In $\text{NH}_3\text{--HCl--(H}_2\text{O)}_2$, the second H_2O molecule significantly contributes to favor the ion pair form over the hydrogen bond form just as does the first H_2O . As a joint result of the two water molecules, the hydrogen-bonded structure is no longer stable with respect to the proton transfer as shown by the decreasing potential energy with $r(\text{H--Cl})$. The potential energy minimum is shifted to $r(\text{H--Cl}) = 1.861 \text{ \AA}$, corresponding to the ion pair structure with the proton completely transferred from HCl to NH_3 . In $\text{NH}_3\text{--HCl--(H}_2\text{O)}_3$, the ion pair structure becomes increasingly more stable than in $\text{NH}_3\text{--HCl--(H}_2\text{O)}_2$, as shown by the more sharply decreasing potential energy with $r(\text{H--Cl})$. The potential minimum in $\text{HCl--NH}_3\text{--(H}_2\text{O)}_3$ is shifted to $r(\text{H--Cl}) = 1.938 \text{ \AA}$. All of these findings suggest that the ion pair structure becomes increasingly more stable as water molecules are added.

Note that there is only a single minimum on the potential energy surface along the proton-transfer pathway in any of $\text{HCl--NH}_3\text{--(H}_2\text{O)}_n$, either at the hydrogen bond or ion pair equilibrium structure. There is no potential energy barrier to separate two minima, one corresponding to the hydrogen bond structure and the other to the ion pair structure.

Harmonic Frequencies. Table 4 presents the harmonic frequencies and infrared intensities of the smaller clusters, $\text{NH}_3\text{--HCl}$ and $\text{NH}_3\text{--HCl--H}_2\text{O}$, with all of the intramolecular modes correlated by the monomer vibrations of NH_3 , HCl , and H_2O . Table 5 presents the harmonic frequencies and infrared intensities of the larger clusters, $\text{NH}_3\text{--HCl--(H}_2\text{O)}_2$ and $\text{NH}_3\text{--HCl--(H}_2\text{O)}_3$, with all of the intramolecular modes correlated by the monomer vibrations of NH_4^+ , and H_2O . The intermolecular harmonic frequencies and infrared intensities are given in the footnotes of Tables 4 and 5. The calculated harmonic vibrational frequencies and infrared intensities of the monomers, NH_3 , HCl , H_2O , and NH_4^+ , are also listed in the two tables along with the available experimental harmonic frequencies in parentheses.^{30,35–37}

The calculated harmonic frequencies and infrared intensities for the monomers are in good agreement with the experimental values. No experimental harmonic frequencies for the gas-phase free NH_4^+ ion are available for comparison. However, the fundamental frequencies for NH_4^+ , determined from the infrared spectra of solid ammonium metavanadate (NH_4VO_3),³⁷ indicate that the calculated harmonic frequencies for NH_4^+ agree

TABLE 5: Harmonic Vibrational Frequencies (in cm^{-1}) and Infrared Intensities (km/mol) of $\text{NH}_3\text{--HCl--(H}_2\text{O)}_2$ and $\text{NH}_3\text{--HCl--(H}_2\text{O)}_3$ Correlated by Intramolecular Vibrational Modes for NH_4^+ and H_2O^a

monomer	mode	isolated monomers		$\text{NH}_3\text{--HCl--(H}_2\text{O)}_2$		$\text{NH}_3\text{--HCl--(H}_2\text{O)}_3$	
		freq	IR int	freq	IR int	freq	IR int
NH_4^{+b}	ν_1 sym str	3414 (3115)	0	3401	59	3441	11
	$\nu_2(e)$ deg def	1734 (1638)	0	1700	60	1728	2
				1731	2	1728	2
	$\nu_3(t)$ deg str	3548 (3250)	195	2419	2108	2771	1577
				3497	220	3571	166
				3617	582	3571	166
	$\nu_4(t)$ deg def	1496 (1398)	155	1335	45	1331	153
				1521	77	1555	80
				1567	297	1555	80
H_2O^c	ν_1 sym str	3884 (3832)	13	3638	447	3698	482
				3631	191	3674	392
						3674	403
	ν_2 antisym str	4003 (3943)	63	3968	64	3969	10
				3968	146	3968	156
						3968	156
	ν_3 bend	1629 (1648)	57	1662	71	1671	104
				1669	64	1659	53
						1659	53

^a Experimental harmonic frequencies for the monomers are given in parentheses. Intermolecular frequencies and IR intensities are listed in Supporting Information. ^b Experimental fundamental frequencies measured for NH_4^+ in solid ammonium metavanadate (NH_4VO_3), from ref 37. ^c Experimental harmonic frequencies for H_2O are from ref 36.

very well with the experiment. Note that fundamental frequencies are typically 90% of the corresponding harmonic frequencies.

It is not surprising that most of the harmonic frequencies of intramolecular modes for the two smaller clusters, $\text{NH}_3\text{--HCl}$ and $\text{NH}_3\text{--HCl--H}_2\text{O}$, remain nearly the same as those for the isolated monomers. This is consistent with the fact that the two clusters exist as intermolecular complexes without significant changes in valence bonding from the isolated monomers. However, there is one major exception which involves the HCl stretching mode (ν_1). The HCl stretching frequency undergoes a red shift of 563 cm^{-1} in $\text{NH}_3\text{--HCl}$ from a frequency of 3091 cm^{-1} for free HCl , along with a sharp enhancement in IR intensity. The red shift in ν_1 (HCl) continues as the first water is added to the $\text{NH}_3\text{--HCl}$ complex with a further enhancement in IR intensity. This is consistent with the successive weakening of the HCl bond as it forms clusters with NH_3 and H_2O . Because of the predicted large frequency shift and intensity enhancement, the ν_1 (HCl) mode for the two clusters may be of great interest to experimentalists who plan to conduct a spectroscopic search for the clusters. This is particularly true because the frequency, 2528 cm^{-1} for $\text{NH}_3\text{--HCl}$ or 1901 cm^{-1} for $\text{NH}_3\text{--HCl--H}_2\text{O}$, is considerably far from all other frequencies of either cluster and is highly IR active.

The harmonic frequencies of the larger clusters, $\text{NH}_3\text{--HCl--(H}_2\text{O)}_2$ and $\text{NH}_3\text{--HCl--(H}_2\text{O)}_3$, are different from those of the smaller clusters. The intramolecular frequencies become difficult to correlate with the frequencies of the isolated NH_3 , HCl , and H_2O , but are easily correlated with the isolated NH_4^+ and H_2O . This can be regarded as strong evidence for the formation of the NH_4^+ ion in the clusters. As expected, on the other hand, the frequencies involving NH_4^+ and H_2O in the clusters are not exactly the same as those of isolated monomers. The differences can be interpreted as the frequency shifts from the pure ion and water to those in the clusters, revealing the strong interactions between the ion species and H_2O in the clusters. The largest frequency shifts appear to be related to the reduction of

symmetry regarding the NH_4^+ unit in the clusters from the isolated ion. For example, the 3-fold degenerate stretching mode $\nu_3(t) = 3548 \text{ cm}^{-1}$ for NH_4^+ is split into 2419, 3497, and 3617 cm^{-1} in $\text{NH}_3\text{-HCl-(H}_2\text{O)}_2$ and 2771, 3571, and 3571 cm^{-1} in $\text{NH}_3\text{-HCl-(H}_2\text{O)}_3$. The frequency with the largest red shift, 2419 cm^{-1} in $\text{NH}_3\text{-HCl-(H}_2\text{O)}_2$ or 2771 cm^{-1} in $\text{NH}_3\text{-HCl-(H}_2\text{O)}_3$, is assigned to the antisymmetric stretching mode corresponding to the transfer of a proton from NH_4^+ to Cl^- , which is an exact reversal of the proton transfer from HCl to NH_3 . Note that the largest red shift also comes with the largest enhancement in IR intensity. This is similar to the HCl stretching in the smaller clusters where HCl is hydrogen-bonded to NH_3 .

The H_2O molecules in the clusters are all oriented according to the argument for favorable electrostatic interactions. No significant changes in frequency would be anticipated for H_2O in the clusters from the isolated H_2O molecule. Indeed, most of the frequencies associated with H_2O in the clusters, particularly in $\text{NH}_3\text{-HCl-H}_2\text{O}$, change very little from those of the isolated H_2O molecule. However, large red shifts in frequency are seen for the symmetric stretching mode (ν_1) of H_2O in the larger clusters in which the ions NH_4^+ and Cl^- exist. The large red shifts also come with sharp enhancements in IR intensity. We may conclude that the H_2O molecules not only have a strong effect on $\text{NH}_3\text{-HCl}$ in the clusters, thereby leading to a proton transfer from HCl to NH_3 and the formation of NH_4^+ and Cl^- , but they are in turn strongly affected by the ions formed. The mutual interactions between H_2O and $\text{NH}_3\text{-HCl}$ might be closely related to nonideal behaviors of aqueous solutions. The continuum models based upon the SCRf theory do not provide the detailed information about solvent-solute effects as described above.

The number of intermolecular vibrational modes increases sharply with the number of monomers present in the cluster. There are 5, 11, 17, and 23 intermolecular vibrations for the clusters with the number $n = 0, 1, 2, 3$ of H_2O , respectively. All of these frequencies are lower than those for the intramolecular modes.

4. Conclusions

We have investigated the gas-phase proton-transfer reaction of ammonia-hydrogen chloride and the effect of first three water molecules by high level ab initio calculations on the molecular clusters $\text{NH}_3\text{-HCl-(H}_2\text{O)}_n$ ($n = 0, 1, 2, 3$). We have calculated the equilibrium structures, binding energies, and harmonic frequencies of the clusters as well as the potential energy surfaces along the proton-transfer pathway of ammonia-hydrogen chloride at the MP2 level with the extended basis set 6-311++G(d,p). We have found that, either without water or with one water molecule, the ammonia-hydrogen chloride system exists as hydrogen-bonded, with hydrogen chloride acting as the hydrogen bond donor and ammonia as the acceptor. With two or three water molecules, the system becomes an ion pair resulting from complete transfer of a proton from hydrogen chloride to ammonia. We have provided a detailed analysis of the potential energy surfaces along the proton transfer pathway in order to determine the effect of the water molecules. The introduction of water molecules into the system increases the stability of the ion pair over the hydrogen-bonded form. The first water molecule is not enough to stabilize the ion pair, but it results in a flatter potential energy pathway for the proton transfer. The second water molecule produces additional stabilization energy which helps fully stabilize the ion pair. The third water molecule contributes to further stabilize the ion pair.

We have also carefully examined the intramolecular harmonic frequencies and infrared intensities of the clusters. This provides further evidence in support of the transition from the hydrogen bond to the ion pair structure as the water molecules are progressively introduced. On the basis of these results, we conclude that ammonium chloride might be formed by the gas-phase reaction of hydrogen chloride with ammonia in the presence of adequate water vapor.

The presence or absence of water appears key to understanding both the microwave experiment of Legon and co-workers^{8,9} and the interdiffusion experiment with the HCl and NH_3 vapors.^{6,7} The microwave experiment was carried out with the vapor from dry ammonium chloride crystals and the interdiffusion experiment was carried out with the vapors from aqueous NH_3 and HCl solutions. In the former, only pure $\text{NH}_3\text{-HCl}$ was involved and, as a result, a simple hydrogen-bonded structure was found. In the latter, water vapor was unavoidable and so the ionic ammonium chloride particles were produced.

Acknowledgment. This work was supported by a Type G grant of Petroleum Research Fund of American Chemical Society (PRF grant #30399-GB6) and a Cottrell College Science Award of Research Corporation (CC4121). The author would also like to acknowledge the use of computing facilities at the W. M. Keck Center for Molecular Structures, California State University, Fullerton.

Supporting Information Available: Intermolecular frequencies and IR intensities (1 page). Ordering information is given on any current masthead page.

References and Notes

- (1) Mulliken, R. S. *J. Phys. Chem.* **1952**, *56*, 801.
- (2) Mulliken, R. S. *Science* **1967**, *157*, 13.
- (3) Clementi, E. *J. Chem. Phys.* **1967**, *46*, 3851.
- (4) Clementi, E. *J. Chem. Phys.* **1967**, *47*, 2323.
- (5) Clementi, E.; Gayles, J. N. *J. Chem. Phys.* **1967**, *47*, 3837.
- (6) Mason, E. A.; Kronstadt, B. J. *Chem. Educ.* **1967**, *44*, 740.
- (7) Shakhshiri, B. Z. *Chemical Demonstrations*; University of Wisconsin: 1985; Vol. 2, p 59.
- (8) Goodwin, E. J.; Howard, N. W.; Legon, A. C. *Chem. Phys. Lett.* **1986**, *131*, 319.
- (9) Howard N. W.; Legon, A. C. *J. Chem. Phys.* **1988**, *88*, 4694.
- (10) Latajka, Z.; Sakai, S.; Morokuma, K.; Ratajczak, H. *Chem. Phys. Lett.* **1984**, *110*, 464.
- (11) Brciz, A.; Karpfen, A.; Lischka, H.; Schuster, P. *Chem. Phys.* **1984**, *89*, 337.
- (12) Jasien P. G.; Stevens, W. J. *Chem. Phys. Lett.* **1986**, *130*, 127.
- (13) Chipot, C.; Rinaldi, D.; Rivail, J.-L. *Chem. Phys. Lett.* **1992**, *191*, 287.
- (14) Bacskay, G. B. *Mol. Phys.* **1992**, *77*, 61.
- (15) Corongiu, G.; Estrin, D.; Murgia, G.; Paglieri, L.; Pisani, L.; Suzzi Valli, G.; Watts, J. D.; Clementi, E. *Int. J. Quantum Chem.* **1996**, *59*, 119.
- (16) Barnes, A. J.; Beech, T. R.; Mielke, Z. *J. Chem. Soc., Faraday Trans.* **1984**, *80*, 455.
- (17) Legon, A. C.; Rego, C. A. *J. Chem. Phys.* **1989**, *90*, 6867.
- (18) Legon, A. C.; Wallwork, A. L.; Rego, C. A. *J. Chem. Phys.* **1990**, *92*, 6397.
- (19) Legon, A. C.; Rego, C. A. *J. Chem. Phys.* **1993**, *99*, 1463.
- (20) Miertus, S.; Scrocco, E.; Tomasi, J. *Chem. Phys.* **1981**, *55*, 117.
- (21) Miertus, S.; Tomasi, J. *Chem. Phys.* **1982**, *65*, 239.
- (22) Möller, C.; Plesset, M. S. *Phys. Rev.* **1934**, *46*, 618.
- (23) Binkley, J. S.; Pople, J. A. *Int. J. Quantum Chem.* **1975**, *9*, 229.
- (24) McLean, A. D.; Chandler, G. S. *J. Chem. Phys.* **1980**, *72*, 5639.
- (25) Krishnan, R.; Binkley, J. S.; Seeger, R.; Pople, J. A. *J. Chem. Phys.* **1980**, *72*, 650.
- (26) Clark, T.; Chandrasekhar, J.; Spitznagel, G. W.; Schleyer, P. v. R. *J. Comput. Chem.* **1983**, *4*, 294.
- (27) Nguyen, M.-T.; Jamka, A. J.; Cazar, R. A.; Tao, F.-M. *J. Chem. Phys.* **1997**, *106*, 8710.

(28) Hehre, W. J.; Random, L.; Schleyer, P. v. R.; Pople, J. A. *Ab Initio Molecular Orbital Theory*; Wiley: New York, 1986.

(29) Frisch, M. J.; Trucks, G. W.; Schlegel, H. B.; Gill, P. M. W.; Johnson, B. G.; Robb, M. A.; Cheeseman, J. R.; Keith, T.; Petersson, G. A.; Montgomery, J. A.; Raghavachari, K.; Al-Laham, M. A.; Zakrzewski, V. G.; Ortiz, J. V.; Foresman, J. B.; Cioslowski, J.; Stefanov, B. B.; Nanayakkara, A.; Challacombe, M.; Peng, C. Y.; Ayala, P. Y.; Chen, W.; Wong, M. W.; Andres, J. L.; Replogle, E. S.; Gomperts, R.; Martin, R. L.; Fox, D. J.; Binkley, J. S.; Defrees, D. J.; Baker, J.; Stewart, J. P.; Head-Gordon, M.; Gonzalez, C.; Pople, J. A. Gaussian 94, Revision D.3; Gaussian, Inc., Pittsburgh, PA, 1995.

(30) Hoy, R.; Mills, I. M.; Strey, G. *Mol. Phys.* **1972**, *24*, 1265.

(31) Huber, K. P.; Herzberg, G. *Molecular Spectra and Molecular Structure, IV. Constants of Diatomic Molecules*; van Nostrand Reinhold Company: New York, 1979.

(32) *CRC Handbook of Chemistry and Physics*, 77th ed.; Lide, D. R., Editor-in-Chief, CRC Press: Boca Raton, 1996–1997.

(33) Meot-Ner, M.; Sieck, L. W. *J. Am. Chem. Soc.* **1991**, *113*, 4448.

(34) Goldfinger, P.; Verhaegen, G. *J. Chem. Phys.* **1968**, *50*, 1467.

(35) Duncan, J. L.; Mills, I. M. *Spectrochim. Acta* **1964**, *20*, 523.

(36) Strey, G. *J. Mol. Spectrosc.* **1967**, *24*, 87.

(37) de Waal, D.; Heyns, A. M.; Range, K.-J.; Eglmeier, C. *Spectrochim. Acta* **1990**, *46A*, 1639–1649.